JOURNAL OF MATERIALS SCIENCE **38** (2003) 57–63

Properties of saccharides and saccharide derivatives in the dry and partially hydrated states

H. M. DERBYSHIRE
School of Pharmacy and Pharmaceutical Sciences, De Montfort University, Leicester, LE1 9BH, UK

I. M. GRIMSEY
School of Pharmacy, University of Bradford, BD7 1DP, UK

C. R. BLAND
Napp Pharmaceuticals, Cambridge, CB4 0GW, UK

J. BROADHEAD
AstraZeneca R&D Charnwood, Loughborough, LE11 5RH, UK

K. G. BROCKLEHURST, N. J. MALONE
Laboratory of the Government Chemist, Runcorn, WA7 4QD, UK

G. SMITH*
School of Pharmacy and Pharmaceutical Sciences, De Montfort University, Leicester, LE1 9BH, UK
E-mail: geoff@dmu.ac.uk

This study investigates the correlation (if any) between the surface properties of dry mannitol, sorbitol and glucose, as determined using inverse gas chromatography (IGC) and other techniques, with microwave dielectric analysis of the molecular polarisability of water in the hydrated material. Microwave dielectric analysis of the hydrated material (using a circular resonant cavity) showed a transition (h_t) in the gradient of imaginary permittivity (ε'' at 2.2 GHz) vs. water content for all materials. This transition reflects the appearance of another population of water with enhanced mobility. The gradient below h_t (m_1) reflects the reorientation mobility of water close to the surface of the solid, and therefore provides one measure of the strength of interaction with each material. Estimates for h_t and m_1 parallel the IGC data by giving a rank order of affinity as glucose > mannitol > sorbitol. This link suggests that the molecular properties of water and the strength of interaction with the hydrated material are most certainly governed by the acceptor/donor properties of the surface (as determined by IGC). Moreover, it can be inferred that the presence of mobile water (up to the relatively high levels defined by h_t) does not change the surface energy of the material. © *2003 Kluwer Academic Publishers*

1. Introduction

The interaction of water with pharmaceutical solids occurs in practically all stages of manufacture, from the raw material to the final dosage form [1]. For example, in the wet granulation process, water is added as part of a binder solution that facilitates the formation of free flowing, homogeneous granules for tablet manufacture. The surface properties of the dry powder blend will affect the distribution and properties of water in the system, which in turn will determine the efficacy of the binding solution. Saccharides and saccharide derivatives are a group of compounds that are of particular interest, owing to their extensive use in pharmaceutical development as fillers, binders, diluents/bulking agents and sweeteners [2]. This group is hydrophilic and readily soluble from the crystalline state. It follows that a concentration of water, sufficient to cause monolayer coverage, will simply hydrate the surface of the solid, whereas larger volumes of free water will result in partial dissolution of the surface. Even further additions of water will then fully dissolve the solid to give a concentrated viscous solution. Factors that govern this process of dissolution with increased water content include the surface energy of the solid, the lattice energy of the crystalline material, the solvation free energy for the solvent-solute interaction, and the method/rate

*Author to whom all correspondence should be addressed.

of addition of the solvent. Moreover, the intermediate state of the partially dissolved solid is likely to comprise regions of concentrated solute, interspersed with agglomerated particles. The surfaces of these particles will have undergone varying degrees of dissolution, which will impact on the surface energy of the new surfaces, and there may also be domains of solid in the form of the crystal hydrate. Reaching an understanding of how these materials behave in practice and what factors define the properties of the intermediate state of hydration is therefore a complex task. The approach taken in this paper was to make some correlation between the surface properties of a range of saccharides and saccharide derivatives (i.e., glucose, mannitol and sorbitol) and the molecular mobility of water in the hydrated material.

The surface properties of the dry materials were investigated by inverse gas chromatography (IGC), X-ray photoelectron spectroscopy (XPS), nitrogen gas adsorption (BET surface area), and scanning electron microscopy (SEM). Two techniques were chosen, to investigate surface polarity, because it was not clear a priori whether it is the molecular surface (as characterized by IGC) or the surface volume (as characterized by XPS) that would influence, and therefore correlate with, the properties of water in the wet systems. This is an important question to address. The addition of relatively large amounts of water (as in this study) would necessarily lead to a certain degree of micro-dissolution of the surface. It follows that the properties of the surface defining the nature of the interaction with water may not be that defined by the molecular surface of the dry material (as characterized by IGC). BET was used to characterize the surface area for water interaction, thereby enabling an estimation of the extent of surface saturation by water, and SEM was used to confirm any anticipated changes in surface topography (via micro-dissolution) following the addition of water. All materials were characterized by powder X-ray diffraction, before and after, hydration, to determine whether any changes in solid state properties occur following the addition of water (e.g., the formation of a hydrate).

Inverse gas chromatography (IGC) determines the surface energetics of a powder from the retention behaviour of known volatile liquids and gasses [3, 4]. The surface energetics of a powder surface are determined by the surface chemistry, which in turn is a function of the molecular arrangement at the surface and the exposure of particular groups [5]. IGC operates in the infinite dilution region and measures surface adsorption below monolayer coverage. It is therefore an appropriate technique for investigating the surface wetting of the powders. Earlier work has shown that IGC can discriminate between batches of raw materials that appear equivalent by other techniques [6, 7].

X-ray photoelectron spectroscopy (XPS) is a surface analytical technique which analyses the sample surface to a depth of ~5 nm. All elements, except hydrogen and helium, are detectable by XPS. The relative proportion of elements present at the surface can be deduced from the XPS spectra. Chemical state information is also afforded from chemical shifts within the individual spectral regions. In this study, the technique was used to compare the relative oxygen and carbon content of the surface of each saccharide/derivative and also to detect the presence of any surface impurities. To this end, high resolution C 1s and O 1s spectra were obtained for each material in addition to a full survey scan.

Dielectric relaxation spectroscopy (DRS) provides structural and molecular information about materials through the study of the electric polarisation in time varying electromagnetic fields [8, 9]. Microwave dielectric analysis is particularly suited to the investigation of the molecular properties of water, in hydrated materials, through the study of the polarisability of the water dipole [10, 11]. In this study, the dielectric properties of the hydrated samples were measured at fixed frequencies (615 MHz, 1.4 GHz and 2.2 GHz) using a circular resonant cavity.

The techniques used in this investigation provide complimentary information on the materials under study. By linking information on the surface components of the un-hydrated material (as determined by XPS and IGC) with the dielectric behavior of the hydrated sample, it should then be possible to define relationships between the surface of the dry material and properties of water in the hydrated sample. This insight could provide a means of grading excipients by their surface properties and interaction with water, perhaps giving selection criteria for choosing excipients for granulation, etc.

2. Methods

The powdered materials investigated were anhydrous glucose (Fischer), anhydrous mannitol (Roquette) and anhydrous sorbitol (Roquette).

2.1. Sample hydration

Each material was hydrated using a direct addition technique, involving the addition of a known amount of water ($\rho > 17\ \mathrm{m\Omega \cdot cm}$) dropwise to a known weight of sample (~10 g), whilst mixing in a small rotary mixer (maximum volume 150 ml). The water added to the samples was expressed as g water per g dry powder (g/g). The hydration range was 0–0.25 g/g (the upper hydration level of each of the samples was such that the hydrated materials were still visually solid, and had not formed a viscous solution). The samples were then placed into tarred glass vials (with lids), and sealed with Parafilm®. The samples were then equilibrated for a minimum of 12 h before analysis.

The moisture contents of the samples were determined by loss on drying in a vacuum oven (=8 mbar), at 80°C (for mannitol and glucose) and 40°C (for sorbitol). The sorbitol is dried at a lower temperature as it melts and forms a glass when dried at 80°C. A desorption equation (Equation 1) was then fitted to the mass vs. time profile in order to provide estimates for the total water content of the samples.

$$M(t) = M_{\mathrm{dry}}(h \exp(-t/\tau) - k_{\mathrm{d}}t + 1) \qquad (1)$$

$M(t)$ is the instantaneous total mass of sample at time t (g), M_{dry} is the mass of sample with all the water desorbed (g), h is the relative moisture index ($=\Delta M/M_{dry}$), t is the time (h), τ is the decay time constant (h), and k_d is the (zero order) dissociation time constant (h^{-1}) to account for any slight decomposition of the sample. The determination, by drying, of the amount of water added to each sample concurs with that known to be added to the batch, thereby validating the method of water analysis for individual samples. This approach therefore determines the total water content of each sample (even the monohydrate water that is later reported to form on hydration of the glucose samples) and therefore accounts for the basal water content of the material in addition to the added water. Moreover, measurements on a number of 1 g samples from each 10 g batch provided information on the consistency of mixing within the batch. The homogeneity of water content was within a coefficient of variance of 3–6% ($n = 4$).

2.2. X-ray powder diffraction

200 mg samples (of both the dry, as received, samples and a selection of hydrated materials) were prepared by gentle grinding and introduced into a STOE powder diffraction system. Diffraction spectra were obtained between values of 2theta of 10 to 89.96, with a step of 0.02. A Cu K_α radiation source (of wavelength 1.54060 Å) was used with a 20 kV (5 mA) generator, and a curved Germanium II mono-chromator.

2.3. Inverse gas chromatography

The 'dry' materials (as received) were packed into a silanised glass column and plugged with silanised glass wool. The temperature of the oven was set at 30°C and dry helium passed through the column (at the chosen rate) for at least 24 h to condition the column. The inlet pressure of the Perkin Elmer Autosystem Gas Chromatograph was adjusted so that a constant flow rate of 9–12 ml · min^{-1} was achieved for each column. The flow rate was measured at the beginning and end of each run and found to be constant. IGC probes were pentane, hexane, heptane, octane, ethylacetate, acetone, chloroform, THF, and dichloromethane. The probes were of HPLC grade or equivalent. Each alkane was injected into the column twice, followed by three injections of the polar probes. The duplicate injections of the alkane probes were then repeated to check that the powder surface had not been altered. The method of Schultz and Lavielle [12] was used to determine the dispersive component of the surface free energy (γ_S^D) and the specific component of the free energy of adsorption ($-\Delta G_A^{SP}$) (Fig. 1). The acceptor/donor properties of the surfaces (K_A and K_D) were estimated using the equation developed by Panzer and Schreiber [13]. This equation is based on the Gutmann donor (DN) and modified acceptor (AN*) numbers of the probes (Equation 2).

$$-\Delta G^{SP} = K_A DN + K_D AN^* \quad (2)$$

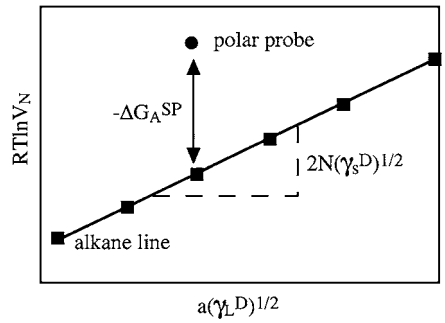

Figure 1 Schematic diagram showing the determination of the specific component of surface free energy.

2.4. X-ray photoelectron spectroscopy

The 'dry' materials (as received) were analyzed using a VG ESCLAB 200 photoelectron spectrometer. The instrument is fitted with a Mg/Al dual anode x-ray source. Mg k_α radiation (1253.3 eV) was used as the excitation source. The background pressure in the analysis chamber was maintained at $\sim 10^{-8}$ mbar during all analyses. All data manipulation was carried out using dedicated VG ECLIPSE software.

2.5. Nitrogen gas adsorption (BET surface area)

The 'dry' materials (as received) were both outgassed and analyzed on a Micrometrics ASAP2400. Outgassing was carried out overnight at room temperature (25°C) and under vacuum of at least 10^{-2} torr. Nitrogen isotherms were produced by adsorbing and desorbing known volumes of nitrogen gas onto the material held at liquid nitrogen temperature. The adsorption process begins at a relative pressure of <0.01, rising to approximately 0.99 in pre-defined steps. Once at the saturation point, the gas was then removed in the same pre-defined way. The primary data for each sample consists of tables giving details of the relative pressures achieved along with the volumes of gas either adsorbed or desorbed at these particular pressures. This isotherm information was then reduced further, using in-house software, to help identify and interpret the porosity information contained within it.

2.6. Scanning electron microscopy

Both the 'dry' materials (as received) and a selection of hydrated materials were characterized by SEM. Hydrated materials were fully dehydrated before measurement by SEM. Samples were mounted onto aluminum stubs and gold coated in a sputter coater (Edwards S150B) to a thickness of ~10 micron. The coated samples were then viewed at 400× magnification in a Leica S430 SEM (beam accelerator voltage was 7.5 kV and the current was 10 pA).

2.7. Resonant cavity dielectric studies

Resonant cavities are high-Q resonant structures, i.e., they have sharp and well-defined resonance peaks (Q, the quality factor, characterizes the sharpness of the resonance). Each cavity has a series of characteristic resonant frequencies. A sample of the material under test,

TABLE I The acceptor and donor properties of the surface, as measured by IGC, expressed in terms of K_A and K_D

	Glucose	Mannitol	Sorbitol
K_A	457	263	152
K_D	1068	659	541

placed inside the cavity, will affect both the resonant frequency and the Q value. The complex permittivity (ε' and ε'') of the sample can then be calculated from the changes in these two parameters using perturbation theory [14] (Equations 3 and 4).

$$\varepsilon' = 1 + 2J_1^2(x_{1m})(\delta f/f_o)(a^2/b^2) \quad (3)$$

$$\varepsilon'' = J_1^2(x_{1m})[(1/Q_1) - (1/Q_o)](a^2/b^2) \quad (4)$$

ε' is the real part permittivity, ε'' is the imaginary part permittivity, $J_1(x_{1m})$ is the roots (x_{1m}) of the first order Bessel function of the first kind, δf is the change in resonant frequency with the sample in the cavity (Hz), f_o is the resonant frequency of the air-filled (empty) cavity (Hz), a is the cavity radius (mm), b is the sample radius (mm), Q_1 is the quality factor of sample in cavity, and Q_o is the quality factor of air filled (empty) cavity.

A cylindrical copper cavity was connected to a HP 8753C vector network analyzer (frequency range 300 kHz–6 GHz). The analyzer was operated in the two port transmission mode and linked to a desktop computer to allow automatic determination of frequency shift and the quality factor for the cavity when the sample was inserted. Hydrated samples were packed into a glass tube of uniform diameter. The density of the sample was recorded and the tube sealed at both ends with Parafilm® to prevent moisture loss. The glass tube was then raised into the copper resonant cavity, with the sample length spanning the cavity (i.e., 50 mm). Measurements (at 25°C) were taken in triplicate, at a selection of resonant frequencies for the cavity (viz. 615 MHz, 1.4 GHz and 2.2 GHz).

3. Results and discussion

3.1. X-ray powder diffraction

The materials were characterized by X-ray powder diffraction (XRPD) in both the dry and hydrated states. Spectra indicated that all materials were predominantly crystalline, with sorbitol showing some amorphous nature. XRPD spectra of mannitol revealed that it was predominantly the (D)-D-mannitol form, when both dry and hydrated. It was also confirmed that sorbitol remained predominantly in the same form following hydration. Conversely, XRPD spectra of hydrated glucose showed additional peaks to the as received 'dry' material, indicating the formation of a hydrate.

3.2. Inverse gas chromatography

The dispersive component of the surface free energy (γ_S^D) was determined by the retention behavior of the alkanes and ranked the materials as mannitol > glucose > sorbitol. The acceptor and donor properties of the surfaces, expressed in terms of K_A and K_D, are shown in Table I. The donor (i.e., basic) properties of the surface were determined by the retention behavior of chloroform and dichloromethane (considered to be acidic probes) and ranked the materials as glucose > mannitol ~ sorbitol. The acceptor properties of the surface were determined by the retention behavior of THF (considered to be a basic probe) and ranked the materials as glucose > mannitol > sorbitol.

TABLE II Estimates of the relative proportion of surface carbon and oxygen atoms as determined by high resolution C 1s and O 1s XPS spectra

	Glucose	Mannitol	Sorbitol
C 1s	53.6 ± 1.9	53.2 ± 1.1	56.3 ± 5.4
O 1s	46.4 ± 1.9	46.8 ± 1.1	43.7 ± 5.5

3.3. X-ray photoelectron spectroscopy

The relative carbon and oxygen content, as determined from the high resolution C 1s and O 1s spectra, of the three material surfaces are given in Table II, expressed as approximate relative ATOM%. Differences between the three materials appear within experimental error and therefore these results were inconclusive.

Modeling of the interactions of THF with mannitol (unpublished data) indicates that the primary interactions of THF with the surface are with the hydrogen atoms on the hydroxyl groups, suggesting that the hydrogen atoms are responsible for surface acidic properties. This observation implies that the chloroform/dichloromethane interacts with the oxygens and that the oxygens are therefore responsible for the basic part of the surface energy. The acidic (K_A) and basic (K_D) character of the surface was ranked as glucose>mannitol>sorbitol (Table I), suggesting that glucose has the higher population of surface hydroxyl groups. It would be expected that an increased proportion of oxygen species, at the surface, would correlate with both increased basicity and increased acidity (as each basic oxygen group would probably carry with it an acidic proton). However, XPS data for the relative proportions of oxygen and carbon does not correlate with the IGC data. This discrepancy may not be surprising given that XPS probes the top 5 nm of the crystal surface, whereas IGC observes only the molecular surface. One would therefore expect the XPS data to be biased to some extent by the whole molecule structure of the materials, in which a 1:1 ratio of carbon to oxygen atoms is expressed. This may explain why the oxygen:carbon ratios for each material were within the experimental limits of error.

3.4. Nitrogen gas adsorption (BET surface area)

Nitrogen adsorption isotherm (BET surface area) analysis of the three samples (as received from the manufacturer) revealed that very low volumes of the gas were absorbed, thereby making it difficult to give an accurate surface area for the samples by this technique. The estimated BET surface areas for mannitol and glucose are $<1\ m^2 \cdot g^{-1}$ and for sorbitol is 1–2 $m^2 \cdot g^{-1}$.

These results and the scanning electron micrographs indicate that either the materials are non-porous, or if porosity is present then the size of the pores are sufficiently large and their corresponding surface area so low that these do not contribute significantly to the overall low surface area. From these BET measurements, monolayer water coverage of each solid was estimated at $\sim 2 \times 10^{-4}$ g/g.

3.5. Scanning electron microscopy

Images of the surface of the samples (see Figs 2 and 3 for example images of glucose) show that the surface of the saccharide is altered following the addition of water (0.1 g/g). Fig. 2 shows that the surfaces of the particles are relatively smooth and non-porous, and there are a number of smaller particles (fines) present. Fig. 3 shows that the addition of water results in a more irregular surface, probably because of microdissolution of the surface of the larger particles and/or adhesion of smaller particles/fines to the larger particles.

3.6. Resonant cavity dielectric studies

The real and imaginary permittivity (ε' and ε'') were calculated (according to Equations 3 and 4) from the shifts in the resonant frequencies of the cavity (viz. 615 MHz, 1.4 GHz and 2.2 GHz). The imaginary part of permittivity (ε'') was found to be more reliable than the real part of permittivity (ε') (at resonant frequencies 615 MHz, 1.4 GHz and 2.2 GHz). In addition, the high frequency resonance measurements (at 2.2 GHz) gave improved signal to noise ratios owing to the fact that the dielectric loss of a hydrated material usually increases as the frequency increases above 0.2 GHz. Estimates for ε'' (at 2.2 GHz) for each material were therefore plotted against water content (Fig. 4), after correction for packing density. An inflection in these plots (termed h_t) was observed for each sample. The inflection was determined by assuming that the relationship between dielectric property and water content is characterised by two straight lines. The two lines of best fit to the data was determined by least-squares minimization, and the error in the estimate for h_t determined from the error in the estimates of the curve fit parameters for the two straight lines. The inflection in the data is believed to be a transition in the properties of water associated with, and surrounding, the material. The transition water content was different for each material (Table III). The precision for the mannitol transition (0.09 ± 0.09 g/g, Table III) was limited because of the small change in gradient. However, measurements using other techniques (NMR, NIR) also give a transition of 0.11 ± 0.01 g/g (unpublished results). The increase in ε'' as a function of water content (below h_t) (termed m_1 in this paper) is also different for each sample (Table III).

In these hydrated materials, an increase in permittivity (Fig. 4) is due largely to the increasing contribution of water to the dielectric loss of the material. Materials which maintain a lower permittivity, on increasing the water content, must therefore have a greater inhibiting effect on the rotation of the water dipole (and/or the correlation between dipoles). The change in the gradient at h_t probably relates to the appearance of another population of water with increased rotational mobility. It is proposed that the gradient below h_t (i.e., m_1) (Table III) is related to the mobility of water and hence the strength of interaction between water and saccharide/saccharide derivative. The gradient (m_1) for glucose is practically zero, suggesting that the mobility of the water below h_t is therefore very restricted. DVS measurements on anhydrous glucose (data not presented) have shown that glucose sorbs water on increasing the relative humidity (RH), but then retains a portion of the water ($\sim$10%) on decreasing the RH to zero. This observation, coupled with XRPD observations comparing anhydrous and hydrated glucose, indicate the formation of a glucose hydrate.

TABLE III Transition moisture content (h_t), gradient below h_t (m_1) and gradient above h_t (m_2), for the saccharide and derivatives determined in the resonant cavity at 2.2 GHz (25°C)

Saccharide/Derivative	h_t (g/g)	m_1	m_2
Glucose	0.12 ± 0.01	0.16 ± 0.14	10.3 ± 0.2
Mannitol	0.09 ± 0.09	2.1 ± 0.1	3.8 ± 0.4
Sorbitol	0.05 ± 0.03	10 ± 1	25 ± 2

Estimates for m_1 (Table III) give a rank order of glucose < mannitol < sorbitol. The trend glucose > mannitol > sorbitol is observed for the values of h_t and therefore the two parameters (m_1 and h_t) are correlated inversely. This result implies that a large value of h_t and a small value for m_1 are reflecting the same property. This is possibly not surprising since the concentration of water above which the appearance of more mobile water is manifest must be defined in some way by the strength of interaction of the water molecules with the material.

The order glucose > mannitol > sorbitol was also observed for the number of acceptor and donor sites, as determined by IGC (Table I). The acidic/basic character of the surface must therefore underpin the way in which water interacts with the sample. What is possibly more surprising is that values for h_t are in excess of those values for monolayer coverage ($\sim 2 \times 10^{-4}$ g/g) and therefore the properties expressed by the dry state may continue to influence the interaction with water up to the concentration h_t. This appears to be the case, despite evidence from scanning electron micrographs shows that microdissolution occurs over this range. It is possible that the value of h_t provides one measure of the extent of microdissolution. Given the link between m_1, h_t and acceptor/donor properties, it follows that the process of microdissolution is also governed by the surface properties determined by IGC. Moreover, it can be inferred that the presence of mobile water (up to the relatively high levels defined by h_t) does not change the surface energy of the material.

The method for preparing the hydrated samples, in this study, has some relevance to that used in wet granulation, i.e., aliquots of water are added to the dry material whilst mixing. The outcome of this study may therefore contribute to our understanding of the granulation process, as well as providing the basis for measuring the interaction of water with materials hydrated

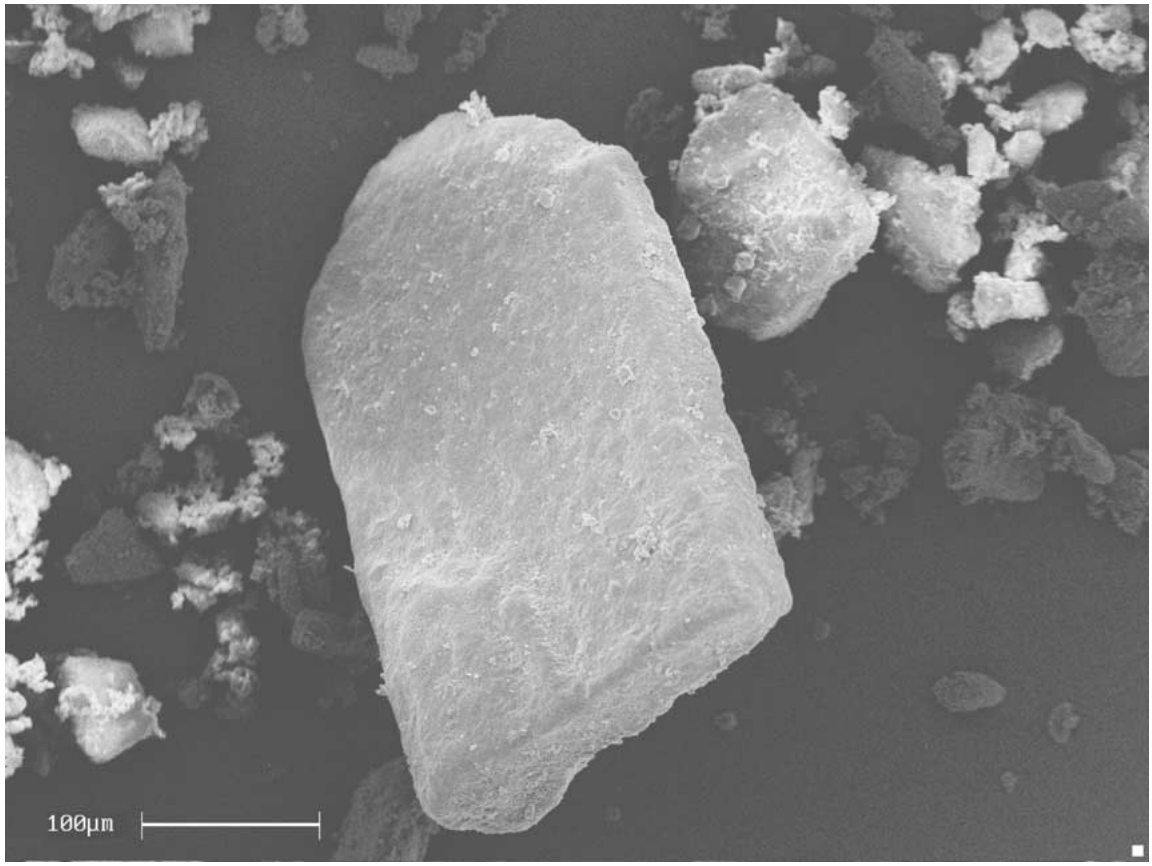

Figure 2 Scanning electron micrograph of glucose as received from the manufacturer.

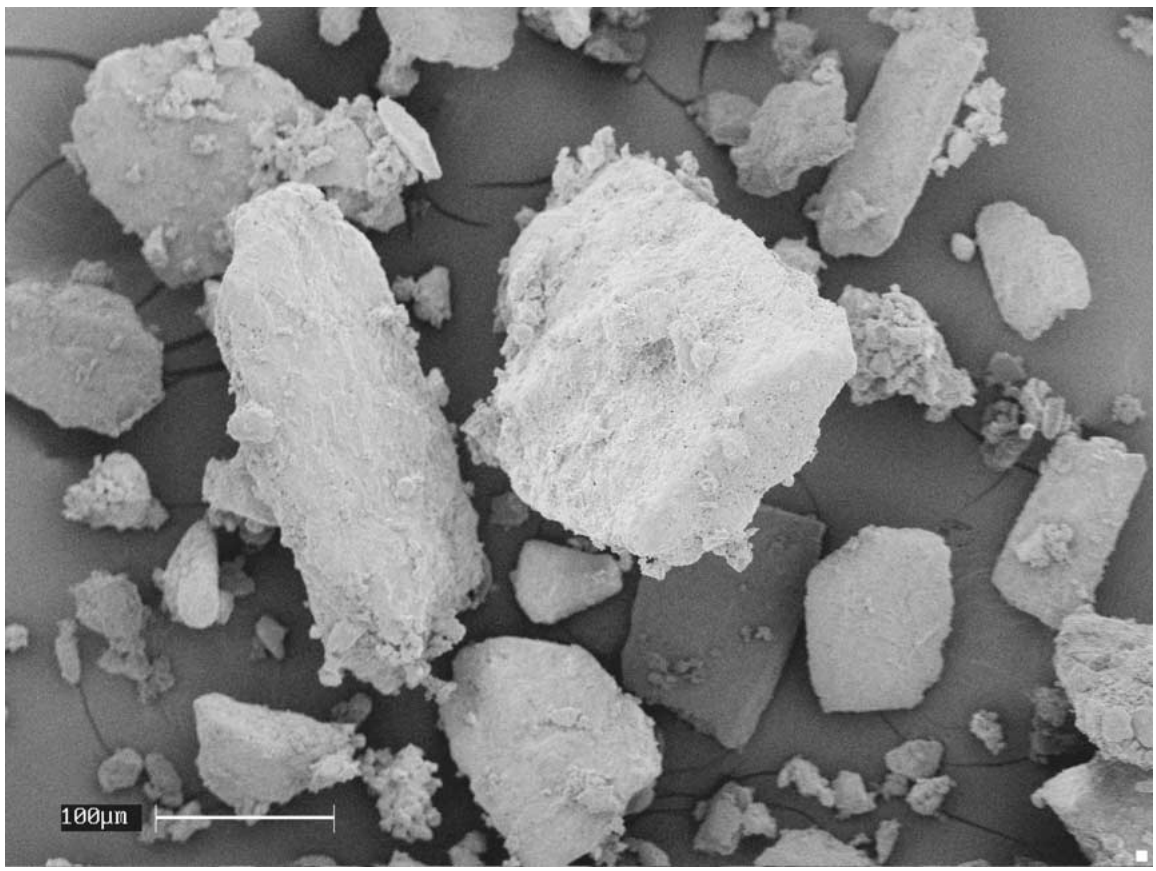

Figure 3 Scanning electron micrograph of glucose hydrated to a level of 0.1 g/g.

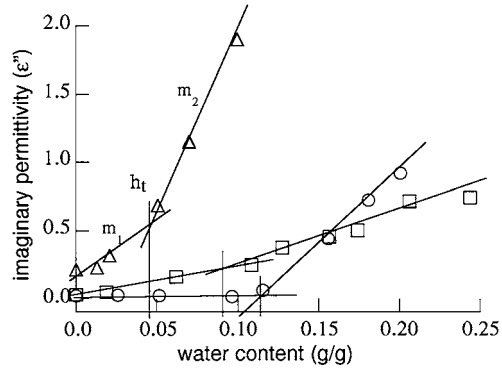

Figure 4 Imaginary permittivity (ε'') of sorbitol, mannitol and glucose as a function of hydration at 2.2 GHz, and 25°C. Each curve exhibits a critical moisture content (h_t) at which the gradient changes from m_1 to m_2. Measurements were made using the dielectric resonant cavity. The plot shows sorbitol (triangle), mannitol (square), and glucose (circle).

by other methods (e.g., exposure to a varying relative humidity). The amount of water required for successful wet granulation has been investigated recently by Miwa *et al*. [15], through the development of a near infrared method. In that study a transition in the measurement response was detected, which was then used as an empirical guide to the maximum amount of water that could be added to the wet granulation mix. However, no information was derived on the mobility of the water or the origins of the transition, in terms of the physical properties of water in relation to the surface properties of the materials studied.

4. Conclusions

This study links the surface acceptor/donor properties of each saccharide/ saccharide derivative with the strength of interaction between water and each material, and may provide information on what surface properties affect the microdissolution of each powder. The results are interesting, in that this type of study may go some way to elucidating the effect of different excipients on the properties of the wet mass in the granulation process. for pharmaceuticals and food stuffs. For example, the dielectric properties of hydrated samples may be predictive of the role played by water as a binder in the formulation. The parameters h_t, m_1 and m_2 could provide useful indices for the prediction of both physical and chemical (e.g., hydrolytic) instability of these systems and any co-additives, as they indicate the mobility of the water in the system (and a lower mobility of water may well provide improved stability).

Acknowledgement

We would like to acknowledge AstraZeneca for funding this research and Dr. Tom Cross (University of Nottingham) for the resonant cavity work.

References

1. M. J. KONTNY, *Drug Dev. Ind. Pharm.* **14** (1988) 1991.
2. A. WADE and P. J. WELLER, in "Handbook of Pharmaceutical Excipients," 2nd ed. (The Pharmaceutical Press, London, 1994).
3. N. HUU-PHOUC, R. P. T. LUU, A. MUNAFO, P. RUELLE, H. NAM-TRAN, M. BUCHMANN and U. W. KESSELRING, *J. Pharm. Sci.* **75** (1986) 68.
4. *Idem., Int. J. Pharm.* **76** (1987) 406.
5. I. M. GRIMSEY, M. SUNKERSETT, J. C. OSBORN, P. YORK and R. C. ROWE, *ibid.* **191** (1999) 43.
6. M. D. TICEHURST, R. C. ROWE and P. YORK, *ibid.* **111** (1994) 241.
7. M. D. TICEHURST, R. C. ROWE, P. YORK and S. K. DWIVEDI, *ibid.* **141** (1996) 93.
8. A. K. JONSCHER, "Dielectric Relaxation in Solids" (Chelsea Dielectrics, London, 1983).
9. S. TAKASHIMA, "Electrical Properties of Biopolymers and Membranes" (Adam Hilger, Bristol, 1989).
10. J. B. HASTED, "Aqueous Dielectrics" (Chapman and Hall Ltd., London, 1973).
11. G. SMITH, *Pharm. Sci.* **1** (1995) 419.
12. J. SCHULTZ and L. LAVIELLE, in "Inverse Gas Chromatography Characterisation of Polymers and Other Materials," edited by D. R. Lloyd, T. C. Ward and H. P. Schreiber (American Chemical Society, Washington DC, 1989) p. 185.
13. H. P. PANZER and U. SCHREIBER, *Macromolecules* **25** (1992) 3633.
14. N. R. GREENACRE, "Measurement of the High Temperature Dielectric Properties of Ceramics at Microwave Frequencies," Ph.D. Thesis, University of Nottingham, Nottingham, 1996.
15. A. MIWA, T. YAJIMA and S. ITAI, *Int. J. Pharm.* **195** (2000) 81.

Received 17 December 2001
and accepted 17 April 2002